9 Computed Tomography in the Concurrent Assessment of Coronary Morphology and Myocardial Perfusion

Ravi K. Sharma, Joao A.C. Lima, and Richard T. George

Abbreviations

CAD	Coronary artery disease
CTA	Coronary computed tomography angiography
CTP	Myocardial computed tomography perfusion
FFR	Fractional flow reserve
ICA	Invasive coronary angiography
MDCT	Multidetector computed tomography
MPI	Myocardial perfusion imaging
NPV	Negative predictive value
PET	Positron emission tomography
PPV	Positive predictive value
SPECT	Single-photon emission computed tomography

R.K. Sharma, MD (✉)
Division of Cardiology, Department of Medicine, Johns Hopkins University, Baltimore, MD, USA
e-mail: rsharm25@jhmi.edu

J.A.C. Lima, MD
Radiology and Epidemiology, Johns Hopkins University, School of Medicine, Cardiology, Baltimore, MD, USA
e-mail: jlima@jhmi.edu

R.T. George, MD
Johns Hopkins University, School of Medicine, Cardiology, Baltimore, MD, USA
e-mail: rgeorge3@jhmi.edu

T.H. Schindler et al. (eds.), *Molecular and Multimodality Imaging in Cardiovascular Disease*, DOI 10.1007/978-3-319-19611-4_9

9.1 Introduction

Rapid advancement in multidetector computed tomography (MDCT) technology has allowed rapid acquisition and assessment of coronary anatomy with high spatial resolution establishing itself as a compelling alternative to invasive coronary angiography (ICA). Coronary MDCT angiography (CTA) is the preferred imaging modality in patients with low- to intermediate-risk probability of coronary artery disease (CAD) given its high sensitivity and negative predictive value in assessment of CAD [1, 2]. However, anatomic imaging does not necessarily implicate that the detected stenosis causes downstream myocardial ischemia [3, 4], a potential therapeutic target using revascularization procedures. Thus, clinical practice guidelines strongly recommend ischemia assessment prior to elective revascularization procedure [5]. The revascularization in patients with concurrent ischemia has been shown to reduce mortality and symptomatic angina. Initial evidence emerges from the Coronary Artery Surgery Study (CASS) registry [6] which reported that patients with multivessel CAD had improved survival with surgical revascularization in the presence of severe ischemia on exercise stress testing, whereas medical therapy was a better approach in patients without significant ischemia. In the nuclear substudy of the COURAGE trial [7], coronary interventions resulted in a reduction in myocardial ischemia burden compared to optimal medical therapy arm, and the reduction of ischemia was associated with mitigation in anginal symptoms and translated into improved prognosis of the patients. The FAME (Fractional Flow Reserve vs. Angiography for Guiding PCI in Patients with Multivessel Coronary Artery Disease) trial [8] demonstrated that fractional flow reserve (FFR)-guided intervention to determine the functional severity of a coronary stenosis resulted in about one-third reduction in mortality and rate of coronary events (myocardial infarctions) compared to anatomic evaluation of stenosis alone.

The relationship between coronary stenosis and myocardial perfusion deficit is complex [3, 4]. The presence and extent of a myocardial perfusion deficit are influenced by multiple factors such as graded severity of stenosis, atherosclerotic burden, microvascular disease, collateral blood flow, as well as endothelial dysfunction [9, 10]. Since the discrepancies occur between the anatomic severity of a lesion and its concurrent hemodynamic effect, functional evaluation of a lesion is essential for clinical decision making, particularly for intermediate severity stenosis. The presence of a hemodynamically significant stenosis confers high risk of future cardiovascular events [11]. From a physician's perspective, it is advantageous to translate these findings into clinical practice in designing preventive or therapeutic interventions for a given patient.

Combination of anatomic and functional imaging offers a solution to the problem with software-based automatic/semiautomatic co-registration of image datasets that is both feasible and reliable. Hybrid imaging systems with CTA as an anatomic arm combined with myocardial perfusion imaging (MPI) in the form of positron emission tomography (PET) or single-photon emission computed tomography (SPECT) allows direct integration of morphologic and functional information. Availability of integrated scanner systems with the capability to perform PET/SPECT imaging in the same setting has made hybrid imaging convenient and logistically feasible. The other alternative is to derive functional information using single

imaging platform with either a single-scan acquisition (CT-FFR) or performing stress myocardial CT perfusion (CTP) imaging. Acquisition of images in the same setting by a single imaging platform is advantageous in routine clinical practice. While CTP has been established as an incremental diagnostic predictor of flow-limiting stenosis [12], CT-FFR that provides hemodynamic information about a focal stenosis from a single image acquisition using complex computational fluid dynamic simulations is currently being investigated for broader applicability [13–15]. These modalities are discussed later in the chapter.

9.2 Background Principles

9.2.1 SPECT and PET-CT Myocardial Perfusion Imaging

Myocardial perfusion SPECT imaging is the most widely used and well-established noninvasive method for assessment of myocardial ischemia. Radionuclide myocardial perfusion imaging uses tracers tagged with radioisotopes that have minimal redistribution and high uptake properties; thereby the concentration of tracer is related to the myocardial blood flow and perfusion [16]. The perfusion pattern reflects the myocardial distribution of the tracer at the time of injection (peak stress) which can be qualitatively and/or quantitatively analyzed [17]. The reported sensitivity for SPECT for detecting >50 % angiographic stenosis is 87 % (range, 71–97 %), whereas the average specificity is 73 % (range, 36–100 %) [18]. With the use of attenuation correction methods, specificity improves especially among patients undergoing exercise stress testing [18]. With PET-MPI, the reported average sensitivity for detecting >50 % angiographic stenosis is 91 % (range, 83–100 %), whereas the average specificity is 89 % (range, 73–100 %) [17].

Initially implemented as an investigative imaging tool to evaluate in vivo quantification of myocardial perfusion and metabolism, PET-MPI has been increasingly utilized as a clinical perfusion imaging modality. PET-MPI in comparison to SPECT imaging has better spatial and contrast resolution. Additionally, well-validated attenuation correction limits the artifacts caused by soft tissue attenuation. This results into improved diagnostic accuracy of PET scanning for detecting obstructive CAD with reported sensitivity and specificity above 90 % [17]. Moreover, PET allows absolute quantification of myocardial perfusion (mL/min/g) that is particularly helpful in assessing the extent of CAD and its downstream perfusion abnormalities in multivessel disease (Fig. 9.1) [19–21]. Recent studies have underlined the clinical significance of absolute myocardial perfusion and have shown that quantitative analysis improves the diagnostic power of detecting CAD disease burden [22–24]. A nonuniform photo attenuation of SPECT imaging results in lower specificity, particularly in obese patients and in women where PET has shown to have improved diagnostic accuracy [21, 25].

Radionuclide perfusion imaging provides information about myocardial perfusion; however, it lacks information about coronary anatomy. Hence, nonobstructive stenoses below the threshold of causing an abnormal perfusion deficit cannot be detected. Simultaneous co-registration of perfusion deficit to a coronary stenosis and coronary artery distribution remain a challenge in the absence of information on

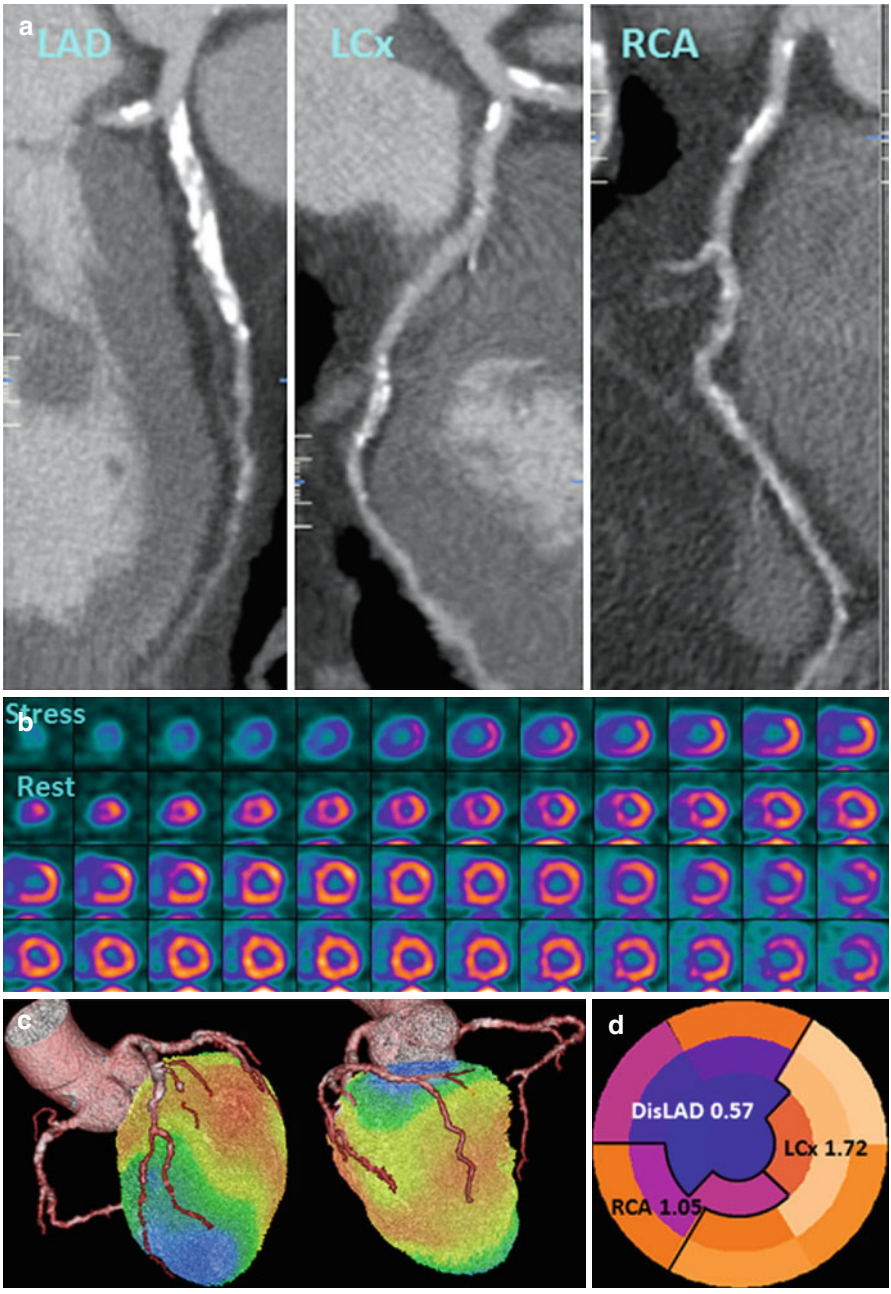
a
LAD
LCx
RCA
b
Stress
Rest
c
d
DisLAD 0.57
LCx 1.72
RCA 1.05

individual coronary anatomy. Standardized allocation of myocardial segment to the individual coronary artery and mental co-registration during scan interpretation may be a simplistic and familiar approach; however, significant anatomic variation exists among standardized vascular "territories" and corresponding coronary segments resulting in disagreement in up to 72 % of the cases [26]. Also, microvascular dysfunction in the absence of epicardial stenosis cannot be ascertained. Thus, accurate spatial localization of myocardial perfusion deficit and designating the individualized coronary artery segment significantly improve the diagnostic value of hybrid imaging and help in devising preventive and therapeutic intervention [17, 27].

9.2.2 Myocardial CTP Imaging

Myocardial CT perfusion imaging was made feasible with the availability of 16-row detector scanner systems [28, 29]. Progression of CT technology to 64-slice scanners allowed the combination of reliable coronary angiogram with stress-induced myocardial CTP technically possible to perform. Previous studies have shown good results with 64-row single-source and dual-source CT scanners [30–33]. However, these systems provide limited coverage of the heart and require cardiac volume acquisitions over several heartbeats, resulting in the more cranial portions of the heart being scanned earlier in time than the more caudal portions causing temporal heterogeneity and making comparisons in signal intensities between the two areas more difficult due to time-related changes in the myocardial contrast concentration [34, 35]. Introduction of wide-coverage (256-row and 320-row) MDCT systems permitted coverage of the entire cardiac volume in a single heartbeat over one gantry rotation. Along with the wide-coverage scan acquisition, prospective cardiac-gated imaging triggered during a specific period of the cardiac cycle (static CTP) mitigated the problem of temporal heterogeneity caused by time attenuation of iodinated contrast concentration in the myocardium. This resulted in significant

Fig. 9.1 Integrated PET/CTA study in a 66-year-old man with obesity, dyslipidemia, and diabetes mellitus. (**a**) Curved multiplanar reconstructions. The proximal LAD shows a long calcified plaque with 85 % stenosis. The LCx artery shows calcified plaques with 47 % stenosis proximally and 77 % stenosis distally. The RCA has a proximal, calcified plaque with 92 % stenosis. The summed stenosis score was 19 in the LAD, 6 in the LCx, and 16 in the RCA. The Duke CAD index was 74. (**b**) Stress and rest myocardial perfusion imaging shows extensive and severe ischemia in LAD territory with transient ischemic dilatation. (**c**) PET/CTA fusion imaging demonstrating that the mid- and basal inferior segments were supplied by a large-dominant LCx in contrast to the standard AHA model. (**d**) $MFR_{regional}$ were 0.57, 1.72, and 1.05 in the in LAD, LCx, and RCA territories, respectively. MFR_{global} was 1.28 (Adapted with permission from Naya et al. [85])

reduction in radiation so as to permit combined coronary CTA and stress myocardial perfusion assessment, providing comprehensive cardiac assessment with acceptable radiation dose. Additionally, faster acquisition has decreased scan times, reducing the amount of contrast material per scan [36].

Contrary to radionuclide myocardial perfusion imaging that uses tracers tagged with radioisotopes, myocardial CTP utilizes iodinated contrast as a perfusion agent. By measuring the concentration over time of the tracer in the myocardium, absolute blood flow in different regions of the myocardium can be estimated [34]. Iodinated contrast has comparable pharmacodynamics properties to gadolinium-based contrast agent used for magnetic resonance perfusion imaging. Iodinated contrast agent is extracted into the extracellular space in a linear relation to time and is excluded from the intracellular space bound by intact cellular membranes [37]. This concentration of iodinated contrast is directly proportional to the measured signal attenuation on a CT image (Hounsfield unit) (Fig. 9.2a, b). It represents a linear relationship between CT-derived metrics and myocardial blood flow and volume, which can be quantitatively analyzed [30, 34]. The extraction fraction of iodinated contrast from intravascular into the extracellular space is paradoxically higher at low blood flow and low at high flows [37]. This is important to consider when quantifying myocardial blood with CT, particularly in regard to correcting for the extraction of iodinated contrast at various flows.

Myocardial rest CT perfusion and delayed enhanced CT are capable of defining myocardial tissue characteristics [38, 39] as well as detecting acute and chronic myocardial infarction and viability [40–42]. However, for the detection of myocardial ischemia, a provocative stress test is necessary to assess for inducible myocardial ischemia. This can be performed by using exercise or dobutamine, both resulting in an increase in heart rate, or using pharmacologic vasodilation with adenosine, dipyridamole, or regadenoson. Since increase in heart rate is not ideal for quality cardiac CT scan acquisition, a vasodilator drug is a preferred stress agent for myocardial CTP with stress images acquired at the time of maximum hyperemia [30, 31, 34]. Adenosine is usually employed as a vasodilator agent and has the advantage of a short half-life that precludes need of reversal agent. However, adenosine administration requires an infusion pump, and side effects include atrioventricular block and bronchospasm [30, 31, 43]. Dipyridamole shares similar pharmacologic properties and side effect with adenosine except having a longer half-life that often requires reversal with aminophylline. Regadenoson is a specific A_{2A} agonist with lower incidence of side effects, primarily in regard to bronchospasm and heart block. Regadenoson's greatest advantage is its ease of administration. It comes in a prefilled syringe with uniform dosing for all patients eliminating drawing up or mixing of drug, infusion pump, and tubing. Regadenoson does cause a slightly higher heart rate than adenosine and dipyridamole [44, 45].

Myocardial stress CTP images can be acquired during a specified time period around the peak of the contrast bolus (static imaging) or serially as the contrast bolus traverses the coronary arteries and myocardial vasculature (dynamic perfusion). For static CTP, images are acquired during the late upslope, peak, and early downslope (Fig. 9.2a) of the contrast bolus and provide data that are qualitative or

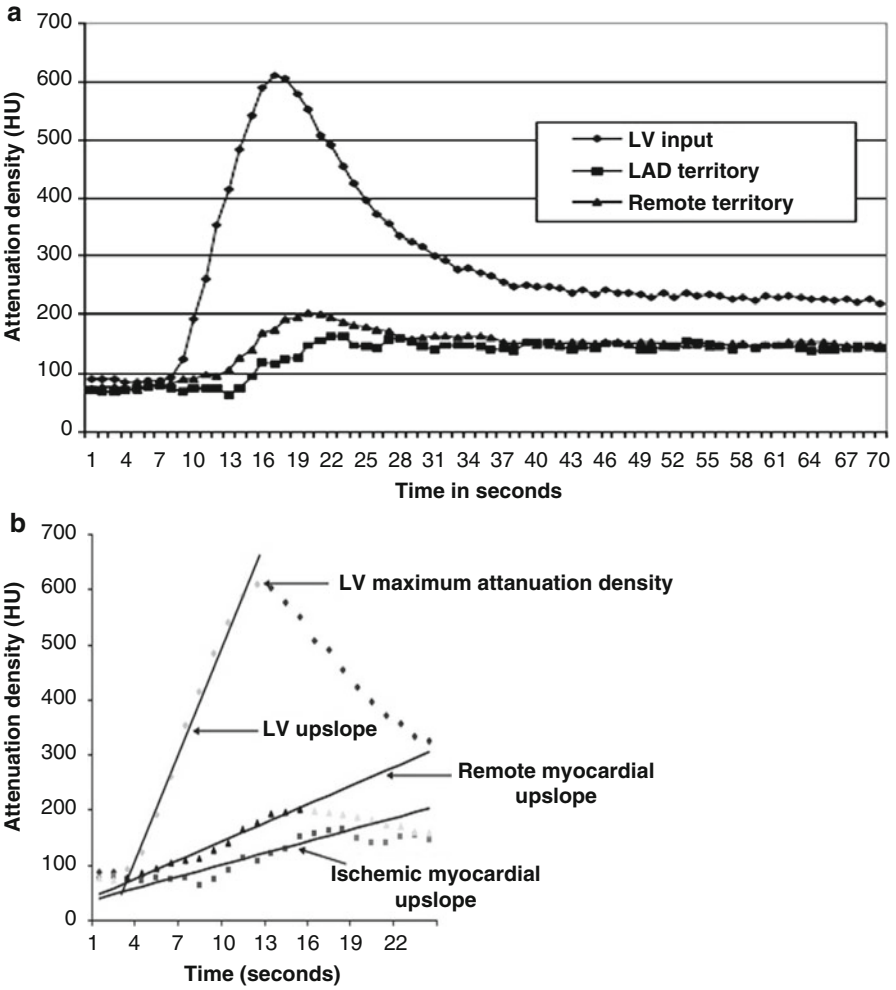

Fig. 9.2 (**a**) Time-attenuation curves for the left ventricle (*LV*), left-anterior descending artery (*LAD*), and remote territories. Attenuation densities over time duration are expressed in Hounsfield units (*HU*). Significant differences are noted in the time-attenuation curves between stenosed LAD territory and remote myocardium. Also note that the LAD territory curve has a delay in onset and time to peak contrast enhancement as well as a lower peak myocardial attenuation density. (**b**) Dynamic MDCT parameters used in the upslope analysis methods. Upslopes of the left ventricular (*LV*) blood pool, remote myocardium, and ischemic myocardium were calculated by applying a best-fit linear regression line from the data points when iodinated contrast first enters the LV cavity to the peak contrast enhancement of the region of interest. Myocardial upslopes were normalized to the LV maximum attenuation density (MUS/LVM ratio) and the LV upslope (MUS/LVUS ratio) (Adapted with permission from George et al. [34])

semiquantitative [34]. Dynamic CTP involves construction of time-attenuation curves of the myocardium and the reference artery allowing calculation of myocardial blood flow and flow reserve [34, 46].

9.2.3 Computed Tomography-Fractional Flow Reserve (CT-FFR)

Recent developments in image-based modeling techniques have allowed accurate segmentation of coronary artery tree and application of computational fluid dynamics within the confines of coronary artery system. Mediated by complex algorithms and calculations applied to the simulated boundary conditions, coronary flow and pressure information can be obtained from rest CTA images. These models can also be used to quantify luminal stenosis and perform flow-pressure simulation models to determine the hemodynamic significance of a lesion, without a necessity of additional scan acquisition or administration of a pharmacologic stress agent.

The CT-FFR method involves derivation of fractional flow reserve (FFR) from anatomic CT data. FFR is defined as a ratio of intracoronary pressure distal to a stenosis and aortic pressure. Principally, segmentation algorithms are applied to create an anatomic model of the coronary artery anatomy followed by mathematical representation of coronary physiology derived using cardiac output, aortic pressure, and microcirculatory resistance. Allometric scaling laws, which analyze the relationship of mass of an object to shape, anatomy, and physiology, are used to define the relation of organ size to flow rate [47]. This enables the computation of coronary flow and pressure. Exploiting these principles, myocardial mass and volume extracted from the coronary CTA data are applied to estimate overall coronary flow under resting conditions. Based on consistent relationship between coronary flow and resistance, total coronary resistance can then be calculated using the coronary flow rate. Extending the mathematical relationship between vessel size and flow rate based on Poiseuille's equation (Q f(dk), where Q is the flow rate through a blood vessel, d is its diameter, and k is a constant), information on the flow rate and relative resistance of the branches arising from the coronary arteries are obtained (Fig. 9.3).

Image segmentation algorithms define the luminal surface of the major vessels and branches, leading up to the vessel diameter limited by the spatial resolution of CTA. Based on the morphometric law, a unique resistance value is then assigned for each coronary artery and its branch outlets. Finally, maximum hyperemic conditions are simulated to model in the effect of adenosine administration (76 % drop from the resting values with intravenous administration of 140 mg/kg/min adenosine) [48] in decreasing the coronary resistance (Fig. 9.4). CT-FFR can then be determined by solving the equations of blood flow for the velocity and pressure fields and normalizing the mean hyperemic pressure field by the average mean hyperemic pressure in the aorta.

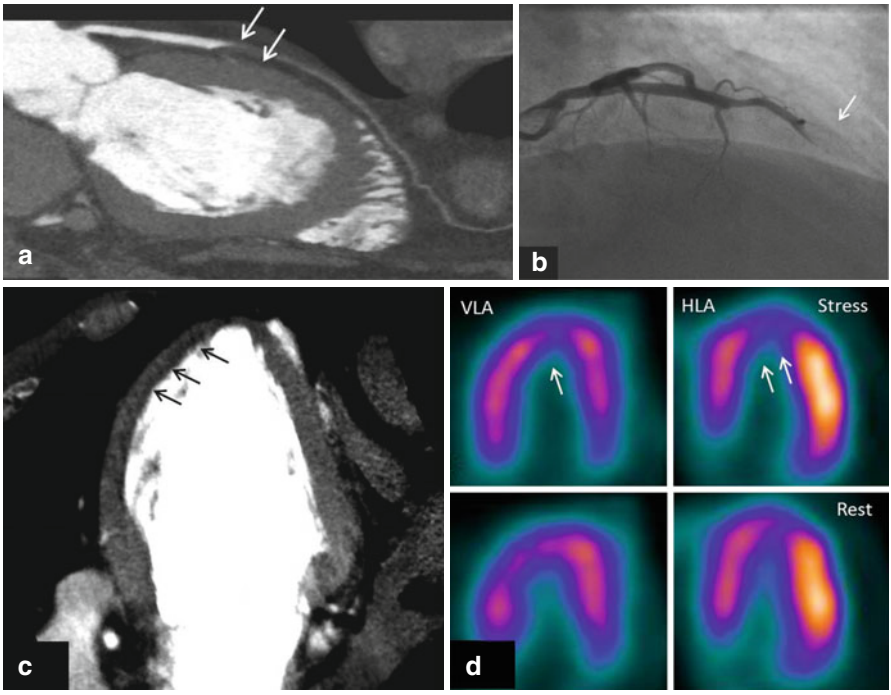

Fig. 9.3 Figures represent combined coronary CTA and myocardial CTP imaging showing flow-limiting stenosis confirmed by invasive coronary angiography and SPECT. CTA (panel-**a**) shows total occlusion of mid-LAD with corresponding CT hypoattenuation (panel-**c**, *black arrows*) involving anterior, anteroseptal, and apical myocardial segments consistent with myocardial CTP deficit. Panel **b** shows complete occlusion (100 % lesion) of mid-LAD on invasive coronary angiography with concurrent SPECT perfusion (panel **d**) defects read in similar myocardial segments as CTP

9.3 Clinical Evidence

9.3.1 Hybrid Imaging

With technical enhancements in image processing software and advent of hybrid scanners, it is possible to perform fusion of the two imaging modalities with simultaneous co-registration of anatomic-physiologic information that enables assigning perfusion territories to a specific stenosis. Clinical data on the diagnostic utility of hybrid imaging is largely restricted to single-center studies. Among intermediate- to high-pretest-likelihood patients, Schaap et al. reported that hybrid SPECT/CTA had a sensitivity of 96 %, specificity 95 %, PPV 96 %, and NPV 95 % [49]. The same group, in a high-risk and known CAD population, also reported that hybrid SPECT/CTA imaging had better diagnostic performance (c-index, 0.96) compared

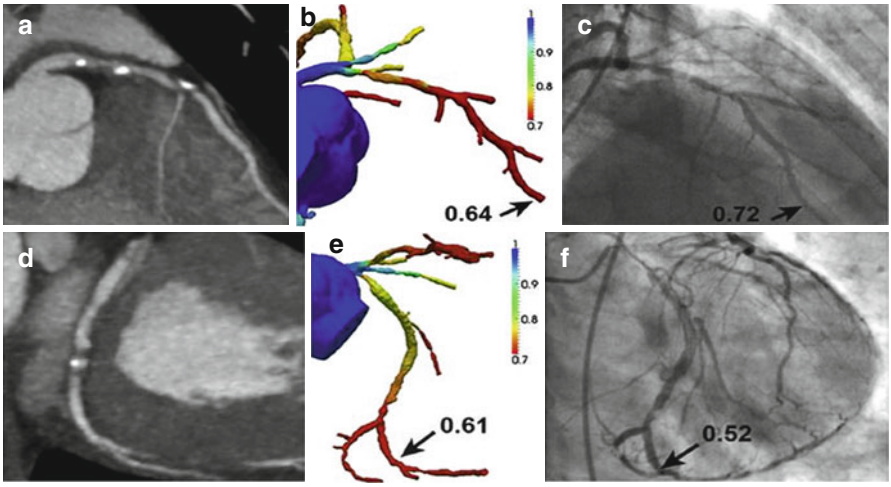

Fig. 9.4 (**a**) CTA demonstrating stenosis in the LAD. (**b**) FFRCTA demonstrates ischemia in the LAD, with a computed value of 0.64. (**c**) ICA with FFR also demonstrates ischemia in the LAD, with a measured value of 0.72. (**d**) CTA demonstrating stenosis in the LCx. (**e**) FFRCTA demonstrates ischemia in the LCx, with a computed value of 0.61. (**f**) ICA with FFR also demonstrates ischemia in the LCx, with a measured value of 0.52 (Adapted with permission from Taylor et al. [13])

to SPECT (0.85) and CCTA (0.90) alone [50]. Another study integrating SPECT and CTA stated PPV of 77 % compared to 31 % for CTA alone in detecting myocardial ischemia [51]. Sato and colleagues [52] reported augmentation of PPV from 69 to 85 % by combining SPECT information to non-evaluable coronary arteries on CCTA.

In a study of 107 patients, $H_2{}^{15}O$ PET/64-slice CTA had a diagnostic accuracy of 98 % with significant improvement in PPV of 96 % for hybrid imaging compared to 76 % for CTA alone [53]. The reference standard was ICA with FFR $\leq$0.80 when feasible. Another study confirmed these findings with reported sensitivity and specificity of 98 % and 91 %, respectively [54]. Danad et al. [55] attested the "gatekeeper" role of hybrid imaging for downstream revascularization and referral for ICA. Of 5 % of the patients with "normal" CTA that were referred for invasive angiography, none had significant CAD. Among the patients that had an equivocal CTA result, 18 % with normal PET-MPI were referred for ICA compared to 71 % in abnormal MPI group, though no coronary revascularization was done in the normal PET-MPI group. Similarly, 72 % patients underwent revascularization for concurrent CTA stenosis and abnormal perfusion versus 26 % with obstructive stenosis ($\geq$50 %) on CTA but normal PET imaging. Hybrid imaging had incremental diagnostic utility in 29 % of the patients, particularly influencing individuals with multivessel disease and/or intermediate-grade stenosis. Thus, combined anatomic-physiologic information derived from hybrid imaging, particularly in the setting of equivocal functional imaging, has been of clinical significance leading to the proportionate decline in false-positive testing. This improved accuracy was most

relevant in the segments perfused by the left circumflex and right coronary artery, affirming the inconsistencies that exist among the myocardial segments perfused by respective coronary vessel [56].

9.3.2 Myocardial CT Perfusion

Numerous single-center studies initially established the diagnostic efficacy of CTP in assessing the flow-limiting stenosis. Using 64-row and 256-row MDCT scanner systems and defining the gold standard as a combination of quantitative coronary angiography and concurrent perfusion abnormalities by SPECT, George et al. on per-patient basis reported the sensitivity, specificity, PPV, and NPV of 86 %, 92 %, 92 %, and 85 % for combined CTA and CTP, respectively. For per-vessel/territory analysis, these corresponding values to detect obstructive stenosis were 79 %, 91 %, 75 %, and 92 %, respectively [30]. Blankstein et al. showed that CTP alone had a sensitivity of 93 % and a specificity of 74 % for the detection of vessels with at least 50 % stenosis and a corresponding SPECT perfusion abnormality [31]. Myocardial CTP has also been compared to invasive FFR in the single-center study by Bettencourt et al. [57] This study enrolled 101 symptomatic patients at intermediate to high risk for CAD. When compared to invasive FFR, myocardial CTP has a diagnostic accuracy of 85 % and a sensitivity, specificity, PPV, and NPV of 89, 83, 80, and 90 %, respectively. Radiation dose was quite low at 5.0 ± 0.96 mSv for the CTA and CTP study combined. Another single-center study examined the added value of CTP over CTA in the diagnosis of in-stent restenosis. Studying 91 patients with suspected in-stent restenosis, Rief et al. [58] tested the diagnostic performance of CTA alone and in combination with CTP. Compared to CTA alone, nondiagnostic rates dropped from 20 to 0 %. There were significant improvements in accuracy, sensitivity, and specificity. Overall diagnostic performance measured by the AUC of the receiver-operator characteristic curve was 0.76 for CTA alone and 0.90 for CTA + CTP ($p < 0.001$).

Following the encouraging results from the single-center experiences, the coronary artery evaluation using 320-row multidetector computed tomography angiography and myocardial perfusion study (CORE320) was an international, multicenter study aimed to establish the incremental diagnostic utility of CTP over CTA against the reference standard of invasive coronary angiography and a corresponding perfusion deficit on SPECT-MPI. The study included patients with prior intracoronary stents and prior myocardial infarction. The study enrolled 381 patients and demonstrated a sensitivity of 94 % and specificity of 64 % for the presence of ≥50 % stenosis by CTA alone to predict the reference standard of combined ICA-SPECT with an AUC (0.84, 95 % CI: 0.79–0.88). The study confirmed significant increase in the patient-based diagnostic accuracy when CTP was added to the CTA (AUC 0.87, 95 % CI: 0.84–0.91). The AUCs for combined CTA-CTP imaging continued to rise to 0.90 for patients without prior myocardial infarction and 0.93 for patients without prior CAD. For the combination of a CTA stenosis ≥50 % stenosis and a CTP perfusion deficit, the sensitivity, specificity, PPV, and NPV values were 80 %, 74 %, 65 %, and 86 %, respectively [12]. A subsequent multicenter study verified that

CTP had a good agreement with SPECT (87 %) imaging and the diagnostic accuracy of CTA (0.69) for detecting a reversible perfusion defect on SPECT improved to 0.85 with the combination of CTP [59]. This study demonstrated that myocardial CTP is non-inferior to SPECT myocardial perfusion imaging for the detection of ≥2 segmental reversible perfusion deficits. Interestingly, CTP has been noted to have a higher sensitivity than SPECT-MPI for detecting of multivessel disease [60].

9.3.3 CT-FFR

CT-FFR derived using rest CTA images has been shown to have improved diagnostic accuracy in predicting lesion-specific ischemia, as determined by invasive FFR. In the Discover-Flow study, Koo et al. [61] in a per-vessel analyses reported better diagnostic accuracy of CT-FFR (AUC, 0.84) compared to CTA stenosis of ≥50 % (AUC, 0.59). On a per-patient basis, CT-FFR had an AUC of 0.87 with stated sensitivity of 94 %, specificity of 82 %, NPV of 0.91, and PPV of 0.85, respectively. In follow-up to the Discover-Flow trial, DEFACTO studied 252 patients with CT-FFR compared to the reference standard invasive FFR. CT-FFR did improve diagnostic accuracy from 64 to 73 %, but overall the trial did not meet its non-inferiority margin. More recently, the Analysis of Coronary Blood Flow Using CT Angiography: Next Steps (NXT) trial evaluated the diagnostic performance of updated iteration of CT-FFR utilizing invasive FFR as a reference standard [14]. In this study, a rigorous quality control mechanism was put in place for CTA and invasive FFR. Of the 365 subjects enrolled with a clinical indication for ICA, 251 subjects made it into the final analysis with 103 studies rejected due to CTA or FFR quality issues. In this study, CT-FFR – on per-patient basis – had an improved diagnostic accuracy with AUC of 0.81 versus 0.53 of CTA alone for detecting flow-limiting stenosis by invasive FFR. CT-FFR had better per-patient sensitivity of 86 %, specificity of 79 %, PPV of 65 %, and NPV of 93 % compared to CTA with corresponding values of 94 %, 34 %, 40 %, and 92 %, respectively. In a meta-analyses to assess the diagnostic performance of CT-FFR, Li and coauthors [62], in a per-patient analysis, reported pooled sensitivity of 89 %, specificity of 71 %, PPV of 70 %, and NPV of 90 % to predict the gold standard of invasive FFR ≤ 0.8. At the vessel level, there was improvement in diagnostic performance of CT-FFR with pooled specificity of 78 % and a comparable sensitivity of 83 %, respectively [62]. Overall, CT-FFR appears to be a robust method to improve the accuracy of CTA to predict the hemodynamic significance. However, CT-FFR has not been extensively tested in patients with prior revascularization or prior infarcts.

9.4 Limitations

Hybrid imaging has significant implications in terms of additional cost, contrast, and radiation exposure. An additional scan may also confer diagnostic delays and logistic challenges that significantly add to patient anxiety and inconvenience.

Therefore, concerted efforts are being made to minimize these problems. Recent years have witnessed significant advances in imaging technology to decrease radiation dose. For SPECT-MPI, introduction of novel small-footprint cardiac scanners armed with solid-state detectors [63] and performance of half-dose perfusion imaging [64] have led to significant reduction in radiation exposure. Optimizing diagnostic yield by using high-efficiency cameras and employing stress-first protocols in individuals with predefined low-intermediate CAD risk have pushed the radiation doses for SPECT imaging to as low as 2.2 mSV [65]. The PET perfusion tracers (i.e., H_2 ^{15}O, $^{13}NH_3$, and ^{82} Rb) construe low radiation doses (1–2 mSv) and may be advantageous for hybrid imaging [66]. Recent advances in CT technology with emphasis on dose reduction techniques like limiting scan length, ECG-gated dose modulation, prospective ECG-triggering, and high-pitch scanning protocols have resulted in significant reductions in effective radiation dose [67]. Additionally, post-processing methods such as iterative reconstruction [68] and availability of next-generation scanners with faster gantry rotation time and wide volume coverage have implied substantial reduction in the amount of radiation during diagnostic testing. With current strategies, a hybrid stress-only SPECT/CTA or PET/CTA studies could be performed with radiation exposure less than or equivalent to invasive diagnostic angiography [69]. Availability of PET perfusion tracers limited by on-site cyclotron is a significant hindrance for performance of PET/CTA hybrid imaging. Although [81] Rb is a generator-based tracer, it requires large patient flow for its commercial viability. Industrial delivery of perfusion tracers with longer half-lives similar to fluorodeoxyglucose (^{18}F) may help alleviate this problem.

MDCT imaging may be influenced by problems arising from image artifacts, lower contrast resolution, contrast dose, and optimal contrast timing. Imaging artifacts are an inherent limitation to CT technology with particular references to artifacts arising out of cardiac motion, beam-hardening, and reconstruction artifacts [70, 71]. Motion artifacts can be further incited by vasodilator stress agents that increase the average heart rate by 20–25 beats/min. These motion artifacts could be avoided by using β-blocker medications and improving the temporal resolution of the scan by using multicycle reconstruction or dual-source CT. Availability of wide-area multi-detector scanner that allows coverage of entire cardiac volume in a single gantry rotation has considerably mitigated this problem [30, 32]. Beam-hardening artifacts are similar to attenuation artifacts in SPECT and arise from the high-attenuation structures (bones and contrast filled ventricular cavity and vessels) that absorb low-energy photons in proximity with the myocardium resulting in low-attenuation streaks. This can be negated by using corrections built into the reconstruction algorithms and by accounting for these artifacts during interpretation of the scan [71, 72].

Strict adherence to imaging protocols to ensure optimum image quality is critical for CT-FFR assessment. CT-FFR requires accurate anatomic framework derived using the image segmentation algorithms that can be influenced by image quality. Hence, the artifacts may have an amplified effect on the calculation of CT-FFR. The presence of coronary calcification and/or stents may result in misrepresentation of CT-FFR. Additional limitations of CT-FFR relate to physiological assumption models that include population as well as patient-specific data. Deduced relationships

relating myocardial mass to total coronary flow, the relative coronary microvascular resistance calculated based on vessel size, or reduction in vascular resistance in response to adenosine-mediated hyperemia will not be consistent among all individuals. Extrapolation of these assumptions to calculate lesion-specific ischemia involves certain degree of variation.

While the results of integrated imaging modalities in assessing lesion-specific or patient-specific ischemia are promising, the data from the published studies are limited and lack uniform reference standard. The applicability and usefulness of combined imaging modalities have not yet been tested beyond clinical trials in the real-world clinical scenario. Currently, there are no data on the cost-effectiveness and improvements in patient outcomes as well as which patient subset will benefit from integrated imaging accounting for cost and radiation dose.

9.5 Prognostic Value

The presence of obstructive CAD and corresponding perfusion defect has a synergistic effect on incidence of adverse cardiovascular events; however, the presence of either conveys an independent prognostic risk. Consistent with this principle, a number of studies have documented improved efficiency of hybrid imaging in predicting adverse cardiovascular risk [11]. In a single-center study of 335 consecutively enrolled patients, Pazhenkottil and coauthors [11] stratified the patients based on CTA stenosis and the presence or absence of matching SPECT perfusion deficit. Combination of abnormal CTA-SPECT translated into worst prognosis with annual major adverse cardiovascular event rate of 21.0 and 6.0 % incidence of death/myocardial infarction. Normal dual-modality scan had lowest major event rate of 2.2 % with 1.3 % risk of death or coronary events. Patient with CTA stenosis and discordant result on MPI had intermediate major adverse event rate of 7.8 % and hard event rate of 2.8 %, respectively. Van Werkhoven et al. [73] had similar findings with annual event rate of 1.0 % (death/MI 0.6 %) in patients with normal CTA (<50 % stenosis) and a normal SPECT-MPI, whereas adverse event rate in patients with obstructive CAD (≥50 %) and corresponding SPECT perfusion abnormality was 9.0 % (death/infarction = 6.0 %). These findings are currently limited to single-center data with relatively smaller cohort size.

Given recent emergence of CTP and CT-FFR technology, outcomes data to assess the prognostic utility is currently in an early stage. Nevertheless, dissociating from the concept of hemodynamically significant stenosis and prognosis, CTA had focused our attention on the significance of total atherosclerotic plaque burden, plaque characteristics, and remodeling status [74]. Studies have projected total atherosclerotic burden as a reliable prognostic marker compared to inducible myocardial ischemia [75, 76]. Integration of these results in improving the risk prediction models in combination with coronary flow reserve and myocardial blood flow and perfusion currently awaits more evidence and data.

9.6 Clinical Perspective

Sequential imaging to obtain anatomic and hemodynamic information can be challenging, particularly in view of establishing "diagnostic yield" of second scan over the first. In a usual clinical setup, additional scan is performed if the result of initial modality is equivocal or if adjunct information is required to define therapeutic strategies. In this regard, individual's pretest likelihood of CAD can help determine the order of the scans. Given the excellent NPV of CTA, anatomic assessment should be performed first in the patients with low to intermediate likelihood of CAD, followed by perfusion imaging in those with obstructive CAD on CTA. Conversely, if the pretest likelihood of CAD is high indicating higher prevalence of obstructive CAD, starting with perfusion imaging may be a better approach, with anatomic imaging being triggered after an abnormal, equivocal, or suboptimal perfusion testing.

Hybrid imaging may be clinically useful in coronary stenosis of moderate severity (30–90 %) where quantitative stenosis may not be a reliable indicator of physiologic significance of a lesion. For such cases, perfusion imaging or CT-FFR can be added to CTA to assess the flow-limiting stenosis. This may be beneficial in a patient with multivessel disease where culprit lesion/s can be identified in the setting of "balanced ischemia." Left main stenosis can also be diagnostically challenging for radionuclide perfusion imaging. The presence of stenosis on CTA and a corresponding large anterior perfusion deficit permit accurate detection of flow-obstructing left main stenosis. In a patient with heavily calcified coronary arteries and uninterpretable coronary segments, perfusion imaging provides useful information about downstream hemodynamic effects, increasing the diagnostic certainty of an obstructive CAD. Quantitative perfusion imaging can also identify microvascular dysfunction, represented by reduced myocardial blood flow in the absence of obstructive epicardial CAD. Finally, dual-modality imaging provides quantitative estimation of the "myocardium at risk" and helps differentiate patient with extensive scar versus significant myocardial ischemia. This is clinically vital so as to guide revascularization approach in those with viable myocardium while avoiding coronary intervention in individuals with no potential for myocardial recovery [77].

9.7 Future Advancement

Rapid evolution of CT technology led by the improvement in temporal and spatial resolution along with post-processing techniques has allowed faster scan acquisition at higher heart rates [78–80]. The role of cardiac MDCT imaging as a comprehensive CAD assessment tool using solo imaging platform, aided by automated and semiautomated analysis software, is currently in sight. It will soon be feasible to obtain enhanced information about coronary morphology and lesion-specific ischemia and/or downstream hemodynamic effects based on single-scan acquisition.

Cardiovascular molecular imaging provides important insights into the biological and vascular processes at the cellular levels. PET-CT imaging has emerged as a powerful imaging tool designed to decipher pathophysiological and metabolic mechanisms of plaque progression and rupture that has led to better understanding of the concept of vulnerable plaque [81–83]. Recent preclinical evidences suggest that macrophage-specific iodine-based contrast agents such as N1177 can noninvasively identify high-risk atherosclerotic features and localize and quantify inflammation in the atherosclerotic plaque [84]. Translation of these promising molecular imaging techniques into the clinical practice remains to be seen.

References

1. Miller JM, Rochitte CE, Dewey M, et al. Diagnostic performance of coronary angiography by 64-row CT. N Engl J Med. 2008;359:2324–36.
2. Arbab-Zadeh A, Miller JM, Rochitte CE, et al. Diagnostic accuracy of computed tomography coronary angiography according to pre-test probability of coronary artery disease and severity of coronary arterial calcification. The CORE-64 (Coronary Artery Evaluation Using 64-Row Multidetector Computed Tomography Angiography) International Multicenter Study. J Am Coll Cardiol. 2012;59:379–87.
3. Uren NG, Melin JA, De Bruyne B, Wijns W, Baudhuin T, Camici PG. Relation between myocardial blood flow and the severity of coronary-artery stenosis. N Engl J Med. 1994;330:1782–8.
4. Di Carli M, Czernin J, Hoh CK, et al. Relation among stenosis severity, myocardial blood flow, and flow reserve in patients with coronary artery disease. Circulation. 1995;91:1944–51.
5. Levine GN, Bates ER, Blankenship JC, et al. 2011 ACCF/AHA/SCAI Guideline for Percutaneous Coronary Intervention. A report of the American College of Cardiology Foundation/American Heart Association Task Force on Practice Guidelines and the Society for Cardiovascular Angiography and Interventions. J Am Coll Cardiol. 2011;58:e44–122.
6. Weiner DA, Ryan TJ, McCabe CH, Chaitman BR, et al. The role of exercise testing in identifying patients with improved survival after coronary artery bypass surgery. J Am Coll Cardiol. 1986;8:741–8.
7. Shaw LJ, Berman DS, Maron DJ, et al. Optimal medical therapy with or without percutaneous coronary intervention to reduce ischemic burden: results from the Clinical Outcomes Utilizing Revascularization and Aggressive Drug Evaluation (COURAGE) trial nuclear substudy. Circulation. 2008;117:1283–91.
8. Tonino PA, De Bruyne B, Pijls NH, et al. Fractional flow reserve versus angiography for guiding percutaneous coronary intervention. N Engl J Med. 2009;360:213–24.
9. Czernin J, Muller P, Chan S, et al. Influence of age and hemodynamics on myocardial blood flow and flow reserve. Circulation. 1993;88:62–9.
10. Schelbert HR. Anatomy and physiology of coronary blood flow. J Nucl Cardiol. 2010;17:545–54.
11. Pazhenkottil AP, Nkoulou RN, Ghadri JR, et al. Prognostic value of cardiac hybrid imaging integrating single-photon emission computed tomography with coronary computed tomography angiography. Eur Heart J. 2011;32:1465–71.
12. Rochitte CE, George RT, Chen MY, et al. Computed tomography angiography and perfusion to assess coronary artery stenosis causing perfusion defects by single photon emission computed tomography: the CORE320 study. Eur Heart J. 2014;35(17):1120–30.
13. Taylor CA, Fonte TA, Min JK. Computational fluid dynamics applied to cardiac computed tomography for noninvasive quantification of fractional flow reserve: scientific basis. J Am Coll Cardiol. 2013;61:2233–41.

14. Norgaard BL, Leipsic J, Gaur S, et al. Diagnostic performance of noninvasive fractional flow reserve derived from coronary computed tomography angiography in suspected coronary artery disease: the NXT trial (Analysis of Coronary Blood Flow Using CT Angiography: Next Steps). J Am Coll Cardiol. 2014;63:1145–55.
15. Nakazato R, Park HB, Berman DS, et al. Noninvasive fractional flow reserve derived from computed tomography angiography for coronary lesions of intermediate stenosis severity: results from the DeFACTO study. Circ Cardiovasc Imaging. 2013;6:881–9.
16. Dilsizian V. SPECT and PET myocardial perfusion imaging: tracers and techniques. In: Dilsizian V, Narula J, editors. Atlas of nuclear cardiology. 4th ed. New York/Heidelberg/Dordrecht/London: Springer; 2013. p. 55–94.
17. Di Carli MF, Dorbala S, Meserve J, El Fakhri G, Sitek A, Moore SC. Clinical myocardial perfusion PET/CT. J Nucl Med. 2007;48:783–93.
18. Klocke FJ, Baird MG, Lorell BH, et al. ACC/AHA/ASNC guidelines for the clinical use of cardiac radionuclide imaging–executive summary: a report of the American College of Cardiology/American Heart Association Task Force on Practice Guidelines (ACC/AHA/ASNC Committee to Revise the 1995 Guidelines for the Clinical Use of Cardiac Radionuclide Imaging). J Am Coll Cardiol. 2003;42:1318–33.
19. Bergmann SR, Fox KA, Rand AL, et al. Quantification of regional myocardial blood flow in vivo with H215O. Circulation. 1984;70:724–33.
20. Hutchins GD, Schwaiger M, Rosenspire KC, Krivokapich J, Schelbert H, Kuhl DE. Noninvasive quantification of regional blood flow in the human heart using N-13 ammonia and dynamic positron emission tomographic imaging. J Am Coll Cardiol. 1990;15:1032–42.
21. Knuuti J, Kajander S, Maki M, Ukkonen H. Quantification of myocardial blood flow will reform the detection of CAD. J Nucl Cardiol. 2009;16:497–506.
22. Kajander SA, Joutsiniemi E, Saraste M, et al. Clinical value of absolute quantification of myocardial perfusion with (15)O-water in coronary artery disease. Circ Cardiovasc Imaging. 2011;4:678–84.
23. Parkash R, deKemp RA, Ruddy TD, et al. Potential utility of rubidium 82 PET quantification in patients with 3-vessel coronary artery disease. J Nucl Cardiol. 2004;11:440–9.
24. Yoshinaga K, Katoh C, Noriyasu K, et al. Reduction of coronary flow reserve in areas with and without ischemia on stress perfusion imaging in patients with coronary artery disease: a study using oxygen 15-labeled water PET. J Nucl Cardiol. 2003;10:275–83.
25. Di Carli MF, Hachamovitch R. New technology for noninvasive evaluation of coronary artery disease. Circulation. 2007;115:1464–80.
26. Javadi MS, Lautamaki R, Merrill J, et al. Definition of vascular territories on myocardial perfusion images by integration with true coronary anatomy: a hybrid PET/CT analysis. J Nucl Cardiol. 2010;51:198–203.
27. Di Carli MF. Hybrid imaging: integration of nuclear imaging and cardiac CT. Cardiol Clin. 2009;27:257–63.
28. Mahnken AH, Bruners P, Katoh M, Wildberger JE, Gunther RW, Buecker A. Dynamic multisection CT imaging in acute myocardial infarction: preliminary animal experience. Eur Radiol. 2006;16:746–52.
29. Garcia MJ, Lessick J, Hoffmann MH. Accuracy of 16-row multidetector computed tomography for the assessment of coronary artery stenosis. JAMA. 2006;296:403–11.
30. George RT, Arbab-Zadeh A, Miller JM, et al. Adenosine stress 64- and 256-row detector computed tomography angiography and perfusion imaging: a pilot study evaluating the transmural extent of perfusion abnormalities to predict atherosclerosis causing myocardial ischemia. Circ Cardiovasc Imaging. 2009;2:174–82.
31. Blankstein R, Shturman LD, Rogers IS, et al. Adenosine-induced stress myocardial perfusion imaging using dual-source cardiac computed tomography. J Am Coll Cardiol. 2009;54:1072–84.
32. George RT, Silva C, Cordeiro MA, et al. Multidetector computed tomography myocardial perfusion imaging during adenosine stress. J Am Coll Cardiol. 2006;48:153–60.
33. Cury RC, Magalhaes TA, Borges AC, et al. Dipyridamole stress and rest myocardial perfusion by 64-detector row computed tomography in patients with suspected coronary artery disease. Am J Cardiol. 2010;106:310–5.

34. George RT, Jerosch-Herold M, Silva C, et al. Quantification of myocardial perfusion using dynamic 64-detector computed tomography. Invest Radiol. 2007;42:815–22.
35. Ho KT, Chua KC, Klotz E, Panknin C. Stress and rest dynamic myocardial perfusion imaging by evaluation of complete time-attenuation curves with dual-source CT. JACC Cardiovasc Imaging. 2010;3:811–20.
36. Hein PA, May J, Rogalla P, Butler C, Hamm B, Lembcke A. Feasibility of contrast material volume reduction in coronary artery imaging using 320-slice volume CT. Eur Radiol. 2010;20:1337–43.
37. Ichihara T, George RT, Silva C, Lima JAC, Lardo AC. Quantitative analysis of first-pass contrast-enhanced myocardial perfusion multidetector CT using a Patlak plot method and extraction fraction correction during adenosine stress. Nucl Sci IEEE Trans. 2011;58:133–8.
38. Schuleri KH, Centola M, George RT, et al. Characterization of peri-infarct zone heterogeneity by contrast-enhanced multidetector computed tomography: a comparison with magnetic resonance imaging. J Am Coll Cardiol. 2009;53:1699–707.
39. Senra T, Shiozaki AA, Salemi VM, Rochitte CE. Delayed enhancement by multidetector computed tomography in endomyocardial fibrosis. Eur Heart J. 2008;29:347.
40. Lardo AC, Cordeiro MA, Silva C, et al. Contrast-enhanced multidetector computed tomography viability imaging after myocardial infarction: characterization of myocyte death, microvascular obstruction, and chronic scar. Circulation. 2006;113:394–404.
41. Mahnken AH, Koos R, Katoh M, et al. Assessment of myocardial viability in reperfused acute myocardial infarction using 16-slice computed tomography in comparison to magnetic resonance imaging. J Am Coll Cardiol. 2005;45:2042–7.
42. Gerber BL, Belge B, Legros GJ, et al. Characterization of acute and chronic myocardial infarcts by multidetector computed tomography: comparison with contrast-enhanced magnetic resonance. Circulation. 2006;113:823–33.
43. Cerqueira MD, Verani MS, Schwaiger M, Heo J, Iskandrian AS. Safety profile of adenosine stress perfusion imaging: results from the Adenoscan Multicenter Trial Registry. J Am Coll Cardiol. 1994;23:384–9.
44. Iskandrian AE, Bateman TM, Belardinelli L, et al. Adenosine versus regadenoson comparative evaluation in myocardial perfusion imaging: results of the ADVANCE phase 3 multicenter international trial. J Nucl Cardiol. 2007;14:645–58.
45. Patel AR, Lodato JA, Chandra S, et al. Detection of myocardial perfusion abnormalities using ultra-low radiation dose regadenoson stress multidetector computed tomography. J Cardiovasc Comput Tomogr. 2011;5:247–54.
46. Christian TF, Frankish ML, Sisemoore JH, et al. Myocardial perfusion imaging with first-pass computed tomographic imaging: measurement of coronary flow reserve in an animal model of regional hyperemia. J Nucl Cardiol. 2010;17:625–30.
47. West GB, Brown JH, Enquist BJ. A general model for the origin of allometric scaling laws in biology. Science (New York, NY). 1997;276:122–6.
48. Wilson RF, Wyche K, Christensen BV, Zimmer S, Laxson DD. Effects of adenosine on human coronary arterial circulation. Circulation. 1990;82:1595–606.
49. Schaap J, Kauling RM, Boekholdt SM, et al. Incremental diagnostic accuracy of hybrid SPECT/CT coronary angiography in a population with an intermediate to high pre-test likelihood of coronary artery disease. Eur Heart J Cardiovasc Imaging. 2013;14:642–9.
50. Schaap J, de Groot JA, Nieman K, et al. Added value of hybrid myocardial perfusion SPECT and CT coronary angiography in the diagnosis of coronary artery disease. Eur Heart J Cardiovasc Imaging. 2014;15:1281–8.
51. Hacker M, Jakobs T, Matthiesen F, et al. Comparison of spiral multidetector CT angiography and myocardial perfusion imaging in the noninvasive detection of functionally relevant coronary artery lesions: first clinical experiences. J Nucl Med. 2005;46:1294–300.
52. Sato A, Nozato T, Hikita H, Miyazaki S, et al. Incremental value of combining 64-slice computed tomography angiography with stress nuclear myocardial perfusion imaging to improve noninvasive detection of coronary artery disease. J Nucl Cardiol. 2010;17:19–26.
53. Gaemperli O, Schepis T, Valenta I, et al. Cardiac image fusion from stand-alone SPECT and CT: clinical experience. J Nucl Med. 2007;48:696–703.

54. Danad I, Raijmakers PG, Appelman YE, et al. Hybrid imaging using quantitative H215O PET and CT-based coronary angiography for the detection of coronary artery disease. J Nucl Med. 2013;54:55–63.
55. Danad I, Raijmakers PG, Harms HJ, et al. Effect of cardiac hybrid 15O-water PET/CT imaging on downstream referral for invasive coronary angiography and revascularization rate. Eur Heart J Cardiovasc Imaging. 2013;15:170–9.
56. Slomka PJ, Cheng VY, Dey D, et al. Quantitative analysis of myocardial perfusion SPECT anatomically guided by coregistered 64-slice coronary CT angiography. J Nucl Med. 2009; 50:1621–30.
57. Bettencourt N, Chiribiri A, Schuster A, et al. Direct comparison of cardiac magnetic resonance and multidetector computed tomography stress-rest perfusion imaging for detection of coronary artery disease. J Am Coll Cardiol. 2013;61:1099–107.
58. Rief M, Zimmermann E, Stenzel F, et al. Computed tomography angiography and myocardial computed tomography perfusion in patients with coronary stents: prospective intraindividual comparison with conventional coronary angiography. J Am Coll Cardiol. 2013;62:1476–85.
59. Cury RC, Kitt TM, Feaheny K, et al. A randomized, multicenter, multivendor study of myocardial perfusion imaging with regadenoson CT perfusion vs single photon emission CT. J Cardiovasc Comput Tomogr. 2015;9(2):103–12.
60. George RT, Mehra VC, Chen MY, et al. Myocardial CT perfusion imaging and SPECT for the diagnosis of coronary artery disease: a head-to-head comparison from the CORE320 multicenter diagnostic performance study. Radiology. 2014;272:407–16.
61. Koo BK, Erglis A, Doh JH, et al. Diagnosis of ischemia-causing coronary stenoses by noninvasive fractional flow reserve computed from coronary computed tomographic angiograms. Results from the prospective multicenter DISCOVER-FLOW (Diagnosis of Ischemia-Causing Stenoses Obtained Via Noninvasive Fractional Flow Reserve) study. J Am Coll Cardiol. 2011;58:1989–97.
62. Li S, Tang X, Peng L, Luo Y, Dong R, Liu J. The diagnostic performance of CT-derived fractional flow reserve for evaluation of myocardial ischaemia confirmed by invasive fractional flow reserve: a meta-analysis. Clin Radiol. 2015;70(5):476–86.
63. Duvall WL, Croft LB, Ginsberg ES, et al. Reduced isotope dose and imaging time with a high-efficiency CZT SPECT camera. J Nucl Cardiol. 2011;18:847–57.
64. Gaemperli O, Kaufmann PA. Lower dose and shorter acquisition: pushing the boundaries of myocardial perfusion SPECT. J Nucl Cardiol. 2011;18:830–2.
65. Einstein AJ, Johnson LL, DeLuca A, et al. Radiation dose and prognosis of ultra-low dose stress-first myocardial perfusion SPECT in patients with chest pain using a high-efficiency camera. J Nucl Med. 2015;56(4):545–51.
66. Namdar M, Hany TF, Koepfli P, et al. Integrated PET/CT for the assessment of coronary artery disease: a feasibility study. J Nucl Med. 2005;46:930–5.
67. Halliburton SS, Abbara S, Chen MY, et al. SCCT guidelines on radiation dose and dose-optimization strategies in cardiovascular CT. J Cardiovasc Comput Tomogr. 2011;5:198–224.
68. Chen MY, Steigner ML, Leung SW, et al. Simulated 50 % radiation dose reduction in coronary CT angiography using adaptive iterative dose reduction in three-dimensions (AIDR3D). Int J Cardiovasc Imaging. 2013;29:1167–75.
69. Husmann L, Herzog BA, Gaemperli O, et al. Diagnostic accuracy of computed tomography coronary angiography and evaluation of stress-only single-photon emission computed tomography/computed tomography hybrid imaging: comparison of prospective electrocardiogram-triggering vs. retrospective gating. Eur Heart J. 2009;30:600–7.
70. Mehra VC, Ambrose M, Valdiviezo-Schlomp C, et al. CT-based myocardial perfusion imaging-practical considerations: acquisition, image analysis, interpretation, and challenges. J Cardiovasc Transl Res. 2011;4:437–48.
71. Mehra VC, Valdiviezo C, Arbab-Zadeh A, et al. A stepwise approach to the visual interpretation of CT-based myocardial perfusion. J Cardiovasc Comput Tomogr. 2011;5:357–69.
72. Kitagawa K, George RT, Arbab-Zadeh A, Lima JA, Lardo AC. Characterization and correction of beam-hardening artifacts during dynamic volume CT assessment of myocardial perfusion. Radiology. 2010;256:111–8.

73. van Werkhoven JM, Schuijf JD, Gaemperli O, et al. Prognostic value of multislice computed tomography and gated single-photon emission computed tomography in patients with suspected coronary artery disease. J Am Coll Cardiol. 2009;53:623–32.
74. Arbab-Zadeh A, Fuster V. The Myth of the "Vulnerable Plaque": transitioning from a focus on individual lesions to atherosclerotic disease burden for coronary artery disease risk assessment. J Am Coll Cardiol. 2015;65:846–55.
75. Mancini GB, Hartigan PM, Shaw LJ, et al. Predicting outcome in the COURAGE trial (Clinical Outcomes Utilizing Revascularization and Aggressive Drug Evaluation): coronary anatomy versus ischemia. JACC Cardiovasc Interv. 2014;7:195–201.
76. Arbab-Zadeh A. Fractional flow reserve-guided percutaneous coronary intervention is not a valid concept. Circulation. 2014;129:1871–8; discussion 1878.
77. Shaw LJ, Hachamovitch R, Berman DS, et al. The economic consequences of available diagnostic and prognostic strategies for the evaluation of stable angina patients: an observational assessment of the value of precatheterization ischemia. Economics of Noninvasive Diagnosis (END) Multicenter Study Group. J Am Coll Cardiol. 1999;33:661–9.
78. Cho I, Elmore K, OH B, Schulman-Marcus J, et al. Heart-rate dependent improvement in image quality and diagnostic accuracy of coronary computed tomographic angiography by novel intracycle motion correction algorithm. Clin Imaging. 2015;39:421–6. doi:10.1016/j.clinimag.2014.11.020. ec 9. pii: S0899-7071(14)00305-2.
79. Tomizawa N, Maeda E, Akahane M, et al. Coronary CT angiography using the second-generation 320-detector row CT: assessment of image quality and radiation dose in various heart rates compared with the first-generation scanner. Int J Cardiovasc Imaging. 2013;29:1613–8.
80. Gassenmaier T, Petri N, Allmendinger T, et al. Next generation coronary CT angiography: in vitro evaluation of 27 coronary stents. Eur Radiol. 2014;24:2953–61.
81. Saraste A, Nekolla SG, Schwaiger M. Cardiovascular molecular imaging: an overview. Cardiovasc Res. 2009;83:643–52.
82. Nahrendorf M, Sosnovik DE, French BA, et al. Multimodality cardiovascular molecular imaging, part II. Circ Cardiovasc Imaging. 2009;2:56–70.
83. Knuuti J, Bengel FM. Positron emission tomography and molecular imaging. Heart. 2008;94:360–7.
84. Hyafil F, Cornily JC, Rudd JH, Machac J, Feldman LJ, Fayad ZA. Quantification of inflammation within rabbit atherosclerotic plaques using the macrophage-specific CT contrast agent N1177: a comparison with 18F-FDG PET/CT and histology. J Nucl Med. 2009;50:959–65.
85. Naya M, et al. Quantitative relationship between the extent and morphology of coronary atherosclerotic plaque and down-stream myocardial perfusion. J Am Coll Cardiol. 2011;58:1807–16.